

Source Localization Using a Current-Density Minimization Approach

Michael I. Miga*, Todd E. Kerner, and Terrance M. Darcey

Abstract—Determining the location of cortical activity from electroencephalographic (EEG) data is important clinically. In this paper, a method is presented which uses the powerful optimization method of simulated annealing in conjunction with a finite-element-based model of the search domain for single-time slice solution of the EEG-inverse problem. The algorithm highlights a new objective function based on the current-density boundary integral associated with the finite-element formulation as the basis for parameter optimization. In two-dimensional experiments in a shallow tank containing saline, single dipoles are located within 2 mm. Simulations studying the algorithms response to structured noise are also presented. The new objective function is shown to take advantage of the natural framework associated with finite-elements and the results suggest that the approach is capable of resolving dipole locations in simulations and experiments.

Index Terms—Dipole, EEG, finite-element, inverse problem, simulated annealing.

I. INTRODUCTION

Over the past three decades, there has been considerable effort directed at localizing and characterizing the electrical sources of cortical brain activity [1]–[6]. If accurate reconstructions of brain activity could be generated, this would allow physicians and researchers to localize critical brain functions and focal pathophysiologies of the brain such as in epilepsy. The primary foci of research have been on the development of appropriate head and source models, in addition to robust methods of equivalent source localization (parameter optimization).

In this paper, we demonstrate and evaluate an equivalent source reconstruction algorithm which utilizes a novel objective function based on surface current density and that combines finite-element models with the powerful optimization technique of simulated annealing. While previously published methods use measured potential differences as the basis for optimization, our approach takes advantage of the finite-element framework by using an objective function based on the current-density boundary integral associated with standard finite-element formulations. Our algorithm also incorporates user-defined target search regions to enable more efficient computation when there is prior knowledge regarding possible source location. For the present purpose of feasibility demonstration, the method is implemented in two dimensions and employs a single time-slice dipole(s) localization approach, although the approach could easily be generalized to three dimensions and more sophisticated source models. A two dimensional physical system consisting of 32 electrodes and a shallow tank containing saline is employed to demonstrate the algorithm's ability to localize a dipole in a system subjected to single-time slice

experimental noise. Simulations are also presented which illustrate the effects of structured noise.

Relevant references with respect to methods of source localization can be found in a review by Koles [7]. Relevant references regarding the finite-element method and simulated annealing in the inverse EEG problem are [8]–[11].

II. METHODS

The model equation describing the quasistatic distribution of electrical potential in a heterogeneous volume subjected to a current source Ω is described by Poisson's equation

$$\nabla \cdot (\sigma \nabla \phi) = \Omega, \quad (1)$$

where σ is conductivity, ϕ is the electrical potential, and the boundary conditions are pure Neumann, $\sigma(\partial\phi/\partial n) = 0$. Equation (1) has been the standard description for the forward-based solution of the electropotential distribution resulting from a dipole in the neuroanatomical context. The treatment of (1) in the finite-element framework begins with the volumetric integration of (1) after multiplication by a spatially continuous weighting function ψ_i

$$\langle \psi_i \nabla \cdot \sigma \nabla \phi \rangle = \langle \psi_i \Omega \rangle \quad (2)$$

where $\langle \cdot \rangle$ indicates integration over the problem domain and ψ_i is the i th member of a complete set of standard finite-element C^0 local Lagrange polynomial interpolants. Applying an integration by parts to the left-hand side of (2) yields the weak form

$$-\langle \sigma \nabla \phi \cdot \nabla \psi_i \rangle = -\oint \hat{n} \cdot \sigma \nabla \phi \psi_i ds + \langle \psi_i \Omega \rangle \quad (3)$$

where \oint denotes integration over the boundary enclosing the problem domain and \hat{n} is the outward-pointing normal direction to this boundary. Spatial discretization of (3) is completed in Galerkin fashion by expanding the unknown potential, ϕ , as a sum of unknown coefficients multiplied by known functions of position, $\phi(x, y) = \sum_j \phi_j \psi_j(x, y)$, when substituted into (3) gives

$$\sum_j \phi_j \langle -\sigma \nabla \psi_j \cdot \nabla \psi_i \rangle = \oint \hat{n} \cdot J \psi_i ds + \langle \psi_i \Omega \rangle \quad (4)$$

where J is the current density ($-\sigma \nabla \phi$). When integrated over the entire domain, (4) can be rewritten in matrix form as $\mathbf{A}\Phi = \mathbf{b}$.

To model current sources within the finite-element mesh, we specify current dipoles (i.e., current source and sink pairs) with unknowns being position (x, y), orientation (θ), and strength (M) for a total of four unknown parameters per source. The distribution of the source to nodes is computed using the linear basis associated with linear triangular finite elements. For source parameter optimization, we employed a simulated annealing algorithm, the details of which were reported by Alotto *et al.* [9]. In our algorithm, we have also incorporated user designated search regions in the case where general localization information may be available. Results not shown here have shown this to be very beneficial especially with multiple sources.

In specifying the objective function for the inverse problem, we have elected a novel strategy with respect to boundary conditions: we specify the measurement potentials found at the electrodes experimentally as Dirichlet conditions in the forward problem and have modeled the source as a current dipole. When enforcing the potentials at the electrodes, the unused Galerkin equations are stored and are used to calculate the magnitude of the current-density boundary integral at the electrodes [i.e., the first term on right-hand side of (4)]. In accordance

Manuscript received May 25, 2001; revised March 8, 2002. The work of T. M. Darcey was supported in part by the National Institutes of Health (NIH) under Grant NS17778. Asterisk indicates corresponding author.

*M. I. Miga is with Vanderbilt University, Department of Biomedical Engineering, Box 351631, Nashville, TN 37235 USA (e-mail: Michael.I.Miga@Vanderbilt.edu).

T. E. Kerner is with the Thayer School of Engineering, Dartmouth College, Hanover, NH 03755 USA.

T. M. Darcey is with the Thayer School of Engineering, Dartmouth College, Hanover, NH 03755 USA, and also with the Dartmouth Hitchcock Medical Center, Lebanon, NH 03756 USA.

Publisher Item Identifier S 0018-9294(02)05785-3.

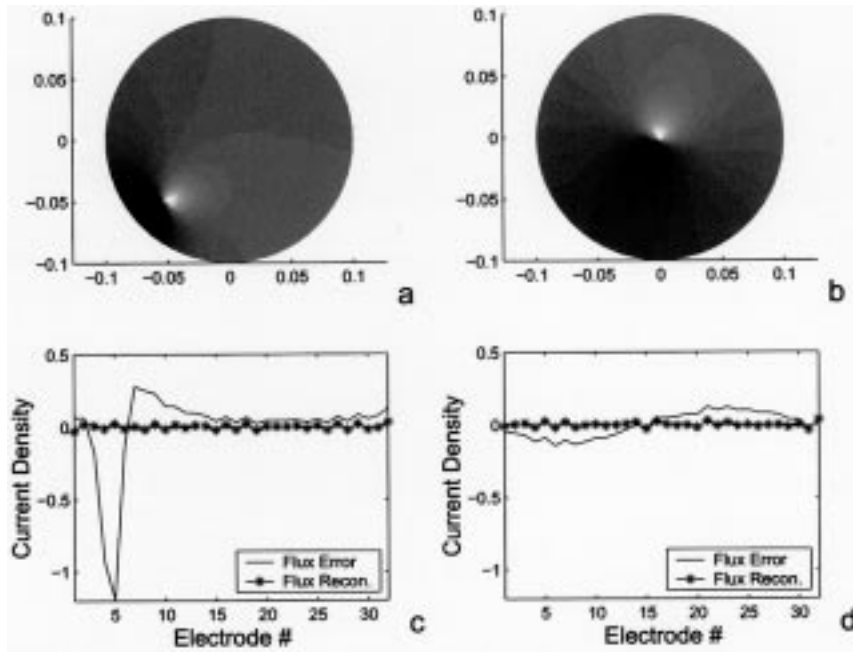


Fig. 1. Single dipole reconstructions for positions at tank (a) boundary and (b) center, respectively, along with their respective current-density integral reconstructions (c) and (d). In (a) and (b) all domains are on a ± 5 -V scale. In (c) and (d), the solid line represents the initial configuration with a source strength of zero while the asterisks represent the current-density boundary integral values at the electrodes with the reconstructed dipole present.

with the inherent boundary conditions, each current density, J , must approach the limit of zero as the dipole estimation improves, hence the boundary integral in (4) must also approach zero. Using this measure, our optimization search is characterized by the minimization of

$$\sum_{l=1}^N C(x_k, y_k, \theta_k, M_k)_l = \sum_{l=1}^N \left(\oint \hat{n} \cdot J_l \psi_l ds \right)^2 \quad (5)$$

where $C(x_k, y_k, \theta_k, M_k)_l$ is the objective/cost function associated with the l th electrode resulting from k dipoles, N is the number of electrodes, J_l is the current density associated with the l th electrode (i.e., J_l is a function of ϕ_j where only contributions in the neighborhood of l are nonzero), and, finally, ψ_l represents the weighting function associated with the l th electrode. This optimization approach avoids issues regarding data differentiation when calculating the current density and is advantageous in three-dimensional (3-D) calculations when using iterative solvers (i.e., only need to compute inverse or precondition matrix once).

To test algorithm performance, a simple testing apparatus consisting of a 32 electrode loop and a shallow circular 20-cm tank filled with saline was used to reconstruct the position, orientation, and magnitude of a simulated EEG source. The source was created by connecting two stainless-steel leads to a dc voltage supply and suspending the leads in the saline tank. Cylindrical heterogeneities were also placed in the tank to study the effects of conductivity. No specific model of the skull conductivity was analyzed in that the focus of this work is on intracranial EEG monitoring. Following the tank experiments, a series of numerical simulations were performed to test reconstruction robustness in the presence of correlated noise. The effects of correlated noise were assessed by positioning a high-magnitude strength dipole approximately 1 cm from the surface electrodes with six surrounding dipoles of lower strength added to confound the surface data in a structured manner. The strength of the surrounding dipoles was chosen to be a fixed percentage level of 5%, 10%, 20%, and 40% of the dominant dipole strength and is referred to as structured noise for the remainder of this paper. It should be noted here that all localization statistics were based on executing the algorithm 20 times for each source reconstruction.

III. RESULTS

Fig. 1(a)–(b) illustrates the reconstruction of dipoles located in positions near the boundary and centrally located within the saline tank, respectively. The accuracy of localization at four different positions within the tank was on average 1.8 ± 0.7 mm, with an orientation error of 1.3 ± 1 deg which is within the certainty that we could physically measure the source location parameters. The magnitudes of the voltages were not equivalent to the experimental ± 20 V, but the localization was quite satisfactory. It is likely that this source magnitude error is associated with the manner in which we discretize our source. Fig. 1(c)–(d) demonstrates that at the global minimum, the conditions noted in (1) are achieved, i.e., the current-density integral at each electrode approaches zero. In results not presented here, the approach was: 1) capable of reconstructing sources to the same accuracy level given above in the presence of heterogeneities; 2) found to be sensitive to mesh resolution; and 3) enhanced when using targeted search regions.

The performance of the algorithm in the presence of large amounts of structured noise (modeled by six interfering dipoles) is shown in Fig. 2(a)–(d) and Table I. Fig. 2(a) shows the potential distribution for a 20% noise level while Fig. 2(d) shows how the reconstruction reduces the peak due to the dominant dipole (circled region above electrode #25). The localization and orientation error for this noise level over a series of 20 inverse calculations was 2.6 ± 0.8 mm and 17.2 ± 5.7 deg., respectively. The results for five different noise levels are listed in Table I.

IV. DISCUSSION AND CONCLUSION

Traditionally, in the EEG inverse problem, the electrode potentials measured are sought by varying the position and orientation of modeled dipoles within the brain. In the new approach described here, the optimization objective is to vary the modeled dipole such that the Neumann boundary condition is satisfied. The results in Fig. 1 illustrate that the approach is feasible and accurate in the idealized experimental

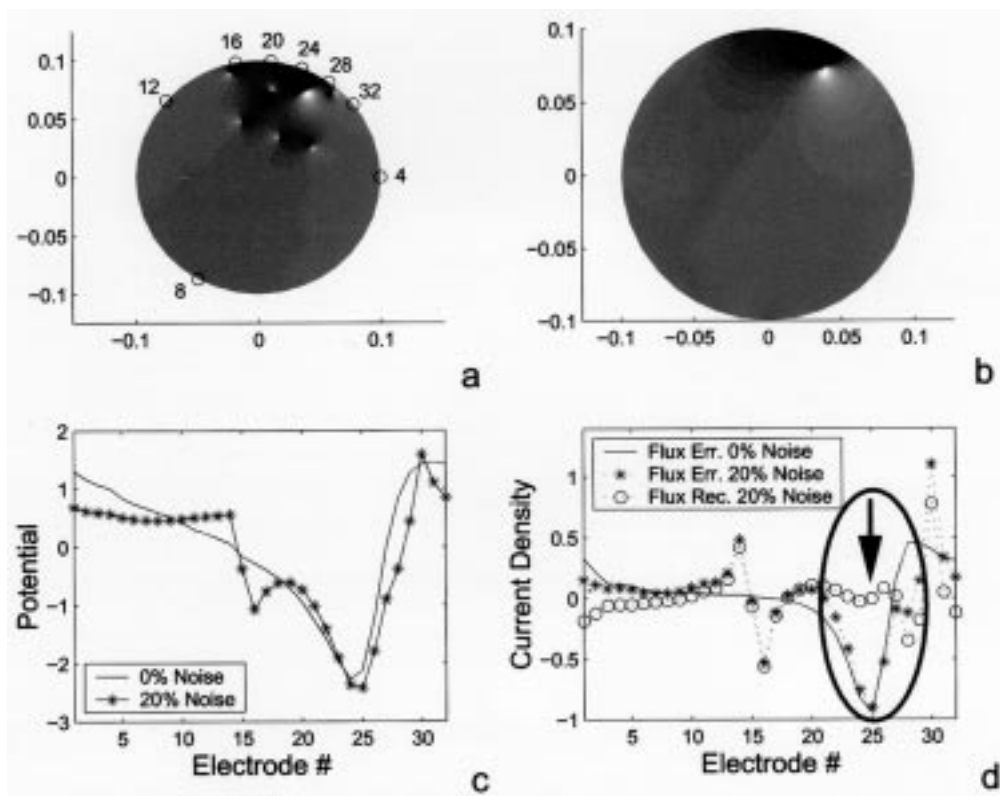


Fig. 2. The results from 20% structured noise dipole reconstruction using a target-region inclusive of all dipoles and a refined grid with: (a) structured noise potential distribution; (b) reconstruction; (c) the difference in electrode potentials between noiseless and 20% noise levels; (d) the current-density integral error associated with 0% and 20% noise levels and the reconstruction effects also shown. All grayscale domains are on a ± 5 -V scale.

TABLE I
LOCALIZATION AND ORIENTATION ERRORS
FOR SOURCE RESOLUTION UNDER
VARYING AMOUNTS OF STRUCTURED
NOISE (MODELED BY SIX LOW-MAGNITUDE
INTERFERING DIPOLES)

Noise %	Localization Error (mm)	Orientation Error (deg.)
0%	1.8 ± 0.8	5.7 ± 4.0
5%	1.9 ± 1.1	17.2 ± 5.7
10%	1.9 ± 1.2	22.9 ± 5.7
20%	2.6 ± 0.8	17.2 ± 5.7
40%	14.2 ± 1.0	28.6 ± 11.5

setup. The results in Fig. 2 demonstrate the robustness of using simulated annealing and finite elements as an optimization methodology. Although not demonstrated specifically here, this arrangement of the inverse problem is favorable to employing finite elements. The formulation allows for the single calculation of the inverse or preconditioner matrix in the case of direct or iterative matrix solvers, respectively, which is a significant reduction in the computational efforts associated with 3-D finite-element solutions.

ACKNOWLEDGMENT

The authors would like to acknowledge the optimization group at the Institute for Fundamentals and Theory of Electrical Engineering of the Technical University of Graz, Graz, Austria, and in particular B. Brandstatter for providing the framework of the simulated annealing algorithm.

REFERENCES

- [1] C. J. Henderson, S. R. Butler, and A. Glass, "The localization of the equivalent dipoles of eeg sources by the application of electric field theory," *Electroencephalogr. Clin. Neurophysiol.*, vol. 39, pp. 117–130, 1975.
- [2] C. C. Wood, "Application of dipole localization methods to source identification of human evoked potentials," *Ann. New York Acad. Sci.*, vol. 388, pp. 139–155, 1982.
- [3] Z. J. Koles, J. C. Lind, and A. C. K. Soong, "Spatio-temporal decomposition of the EEG: A general approach to the isolation and localization of sources," *Electroencephalogr. Clin. Neurophysiol.*, vol. 95, pp. 219–230, 1995.
- [4] I. F. Gorodnitsky, J. S. George, and B. D. Rao, "Neuromagnetic source imaging with FOCUSS: A recursive weighted minimum norm algorithm," *Electroencephalogr. Clin. Neurophysiol.*, vol. 95, pp. 231–251, 1995.
- [5] J. C. Mosher and R. M. Leahy, "Recursive MUSIC: A framework for EEG and MEG source localization," *IEEE Trans. Biomed. Eng.*, vol. 45, pp. 1342–1354, Nov. 1998.
- [6] B. N. Cuffin, "EEG dipole source localization," *IEEE Eng. Med. Biol. Mag.*, vol. 17, pp. 118–121, May-June 1998.
- [7] Z. J. Koles, "Trends in EEG source localization," *Electroencephalogr. Clin. Neurophysiol.*, vol. 106, pp. 127–137, 1998.
- [8] D. Khosla, M. Singh, and M. Don, "Spatio-temporal EEG source localization using simulated annealing," *IEEE Trans. Biomed. Eng.*, vol. 44, pp. 716–723, June 1997.
- [9] P. G. Alotto, C. Eranda, B. Brandstatter, G. Furntratt, C. Magele, G. Molinari, M. Nervi, K. Preis, M. Repetto, and K. R. Richter, "Stochastic algorithms in electromagnetic optimization," *IEEE Trans. Magn.*, vol. 34, pp. 3674–3684, Sept. 1998.
- [10] K. A. Awada, D. R. Jackson, S. B. Baumann, J. T. Williams, D. R. Wilton, P. W. Fink, and B. R. Prasky, "Effect of conductivity uncertainties and modeling errors on EEG source localization using a 2-d model," *IEEE Trans. Biomed. Eng.*, vol. 45, pp. 1135–1145, Sept. 1998.
- [11] L. Zhukov, D. Weinstein, and C. Johnson, "Independent component analysis for EEG source localization," *IEEE Eng. Med. Biol. Mag.*, vol. 17, pp. 87–96, May-June 2000.